January 2009

A planar parasitic array antenna for tunable radiation pattern

Jeong Seongheon

Ha Dohyuk

W. J. Chappell

A Planar Parasitic Array Antenna for Tunable Radiation Pattern

Seongheon Jeong, Dohyuk Ha, and William J. Chappell
Department of Electrical and Computer Engineering, Purdue University
E-mail: {jeong11, chappell@purdue.edu}

Introduction

More than 150 sensor nodes are currently being deployed over the mid-size city of South Bend, IN to monitor sewer flows in our project. We found that RF receivers are often limited by interference in the wireless sensor network. In order to overcome this problem using antenna technology, it is desirable for the nodes to have low-cost beam steering capabilities. Conventional digital-beamforming array antennas use many T/R modules and phase shifters, which result in expensive systems. One way to significantly reduce the cost is to use a single driven element with multiple tunable parasitic elements as radiators. By tuning the termination impedance of the parasitic elements it is possible to adjust the antenna pattern. Many researchers have investigated parasitic arrays over the past few decades [1]-[4]. In this paper, a cross-type parasitic array antenna is designed to tune the radiation pattern which will attenuate incoming interference and improve packet reception. Using only a 5-element planar array allows full 2-dimensional beam steering. The measurement shows that approximately 30 degrees of beam steering can be achieved by terminating parasitic elements with commercial Si-based varactors allowing rapid and automatic adjustment of antenna patterns.

Design and Analysis

The configuration of the proposed parasitic patch antenna is shown in Fig. 1(a). There is a driven element(D) in the center surrounded by four parasitic elements(P) which make strong coupling. Each parasitic element is terminated by a variable impedance. A single slot-fed patch antenna is designed at 2.44GHz and the same antennas are aligned on the right, left, top, and bottom. The design parameters are shown in Fig. 1(b). W and L are the width and length of a patch, respectively. D_x and D_y are the spacing between the driven and parasitic elements, respectively. The patch antennas are designed on 1.575mm-thick Rogers® RO5880 (ε_r=2.2, tanδ=0.0009). The feed line and slot aperture is fabricated on 1.28mm-thick RO3010 (ε_r=10.2, tanδ=0.0023). Each patch has the same size ($W = L =$ 36mm) and is equally spaced from the driven element by 55mm ($D_x = D_y$ =55mm) as shown in Fig. 2.

The mutual coupling between patches is determined by D_x and D_y. This coupling is calculated by HFSS. The reflection coefficient is significantly affected by D_x and D_y. The coupling between the parasitic elements can be negligible in this case. The radiation pattern can be explained by multiplying the element factor with the array factor. The element factor of a single patch antenna is expressed as equation [5]. The array factor of five patch antennas is derived from the M by N planar array formulation as equation (1) [5]. For N=3 and M=3 in this paper, the array factor can be written as equation (2) where I_1 is current on the driven element and I_2, I_3, I_4, and I_5 are current on the parasitic element.

978-1-4244-3647-7/09/$25.00 ©2009 IEEE

$$AF = \sum_{n=1}^{N} I_{1n}\left[\sum_{m=1}^{M} I_{m1} e^{j(m-1)(kd_x \sin\theta \cos\phi+\beta_x)}\right] e^{j(n-1)(kd_y \sin\theta \sin\phi+\beta_x)} \quad (1)$$

$$AF = I_1 + I_2 e^{-j(kd_y \sin\theta\sin\phi+\beta_y)} + I_4 e^{j(kd_y \sin\theta\sin\phi+\beta_y)} + I_3 e^{-j(kd_x \sin\theta\cos\phi+\beta_x)} + I_5 e^{j(kd_x \sin\theta\cos\phi+\beta_x)} \quad (2)$$

These currents are calculated using five-port network theory described in equation (3). Since the parasitic antenna loads are terminated with varactors $Z_c=1/j\omega C$ (for i=2,3,4, and 5), the corresponding voltage is known by $V_i=-Z_cI_i$ (for i=2,3,4, and 5). Therefore, the input impedance is given by equation (4).

$$\begin{bmatrix} V_1 \\ V_2 \\ V_3 \\ V_4 \\ V_5 \end{bmatrix} = \begin{bmatrix} Z_{11} & Z_{12} & Z_{13} & Z_{14} & Z_{15} \\ Z_{21} & Z_{22} & Z_{23} & Z_{24} & Z_{25} \\ Z_{31} & Z_{32} & Z_{33} & Z_{34} & Z_{35} \\ Z_{41} & Z_{42} & Z_{43} & Z_{44} & Z_{45} \\ Z_{51} & Z_{52} & Z_{53} & Z_{54} & Z_{55} \end{bmatrix} \begin{bmatrix} I_1 \\ I_2 \\ I_3 \\ I_4 \\ I_5 \end{bmatrix} \quad (3)$$

$$Z_{in} = \frac{V_1}{I_1} = \frac{-Z_{21}(Z_{11}I_1 + Z_{12}I_2 + Z_{13}I_3 + Z_{14}I_4 + Z_{15}I_5)}{(Z_c + Z_{22})I_2 + Z_{23}I_3 + Z_{24}I_4 + Z_{25}I_5} \quad (4)$$

The termination impedance is implemented by varactors which can be equivalent to parallel resistor and capacitor. The resistor represents the energy loss and the capacitor represents the phase shift, which in turn is used to change the amplitude and phase of the reflected waves.

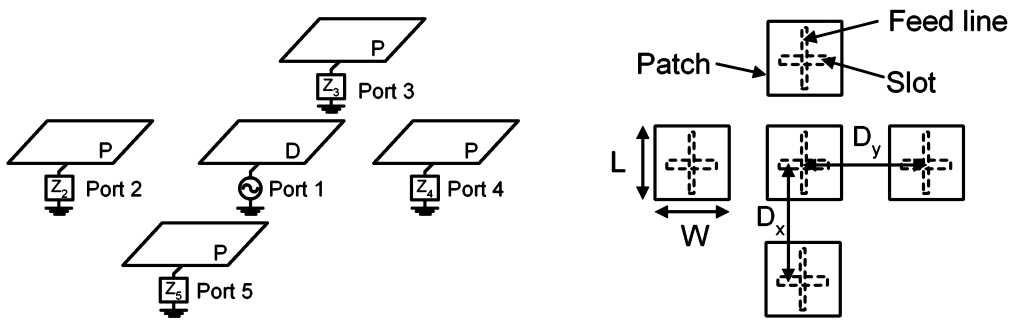

(a) Driven and parasitic patch array (b) Design parameters

Fig.1 Proposed parasitic patch array

(a) Radiating side (b) Feeding side

Fig.2 Fabricated parasitic patch array

Measurement

The fabricated parasitic antenna shown in Fig. 2 was measured in an anechoic chamber. The varactor (BB857) used in the measurement has the capacitance range of 0.5pF to 6.6pF as the voltage changes 28V to 1V, respectively. A continuously tunable radiation pattern is achieved by adjusting these capacitances. As an example, four different cases are given with the detail impedance values as described in Table I. The simulated and measured radiation patterns are in a good agreement as shown in Fig. 3. Simple DC bias tuning can make the beam steerable by approximately 30 degrees. The measured peak gain achieved is 7.8dBi when all parasitic elements are terminated with 0.5pF. The slight frequency shift of reflection coefficient seen in Fig. 4 might come from fabrication error but is less than 2.8%. For our wireless sensor network that this system was developed for, the signal-to-noise ratio was not as defining a metric for packet reception as signal-to-interference ratio (SIR). The system was interference limited and the benefit of the slight adaptively is shown for a typical scenario. If signal and interference are incident as illustrated in Fig. 3(e), SIR increases by 6.4dB as shown in Fig. 5. A reduction in gain due to antenna mismatch becomes less important if the SIR is improved by tuning the radiation pattern.

TABLE I
TERMINATION IMPEDANCE FOR PARASITIC ELEMENTS

	Case 1	Case 2	Case 3	Case 4
Z_1	100Ω , 0.5pF	100Ω , 1pF	100Ω , 2pF	100Ω , 6.6pF
Z_2	100Ω , 0.5pF	100Ω , 0.5pF	100Ω , 0.5pF	100Ω , 0.5pF
Z_3	100Ω , 0.5pF	100Ω , 0.5pF	100Ω , 0.5pF	100Ω , 0.5pF
Z_4	100Ω , 0.5pF	100Ω , 0.5pF	100Ω , 0.5pF	100Ω , 0.5pF

Conclusion and Discussion

A planar cross-type parasitic patch array antenna has been successfully demonstrated to give tunable radiation patterns. Even with readily available commercial varactors, approximately 30 degrees of tunability is achieved. The simulated result is well matched to the measured result. If different varactors were used with an increased capacitance range then the antenna pattern could be tuned more, however more side lobes would also be introduced.

References

[1] R. J. Dinger, "Adaptive microstip antenna array using reactively terminated parasitic elements," *Antennas and Propagation Symp.*, vol. 20, May 1982.
[2] R. J. Dinger, "Reactively steered adaptive array using microstrip patch elements at 4GHz," *IEEE Trans. on Antennas and Propagation*, vol. AP-32, no.8, August 1984.
[3] T. Ohira, "Blind adaptive beamforming electronically-steerable parasitic array radiator antenna based on maximum moment criterion," *IEEE AP-S International Symp.*, vol.2, pp.652-655, June 2002.
[4] Y. Yusuf and X. Gong, "Beam-steerable patch antenna array using parasitic coupling and reactive loading," *IEEE AP-S International Symp.*, pp.4693-4696, June 2007.
[5] C. A. Balanis, Antenna Theory – Analysis and Design, 3rd edition, Wiley, 2006

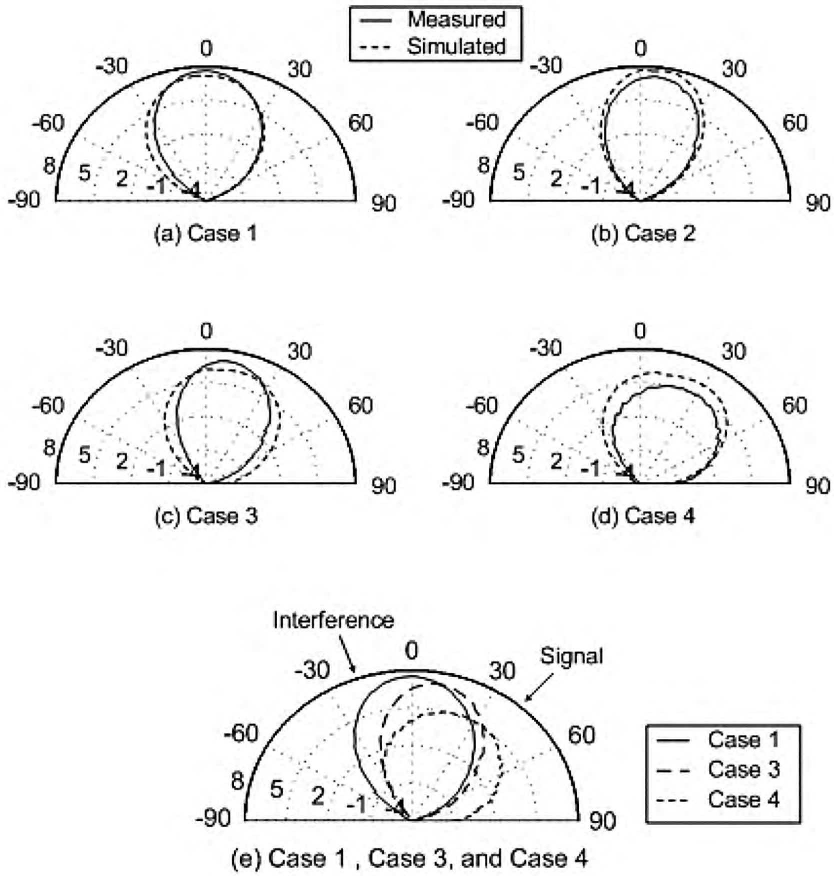

Fig.3 Tunable radiation pattern for different reactive loads

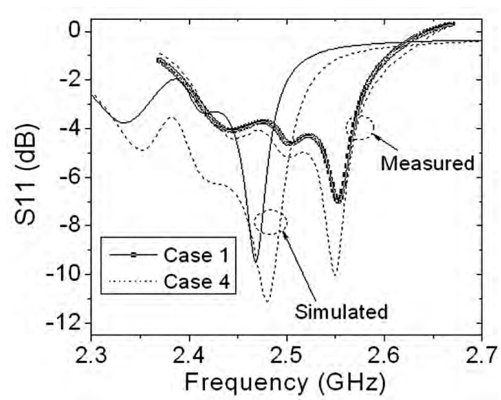

Fig. 4 Reflection coefficient

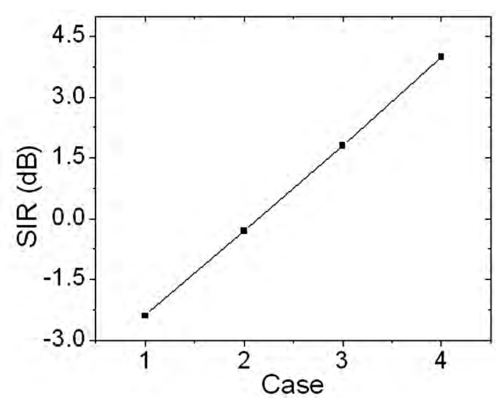

Fig. 5 Signal-to-interference ratio